Portable X-ray fluorescence in stream sediment chemistry and indicator mineral surveys, Lonnie carbonatite complex, British Columbia

Pearce Luck[1] and George J. Simandl[1, 2, a]

[1] British Columbia Geological Survey, Ministry of Energy and Mines, Victoria, BC, V8W 9N3
[2] University of Victoria, School of Earth and Ocean Sciences, Victoria, BC, V8P 5C2
[a] corresponding author: George.Simandl@gov.bc.ca

Recommended citation: Luck, P. and Simandl, G.J., 2014. Portable X-ray fluorescence in stream sediment chemistry and indicator mineral surveys, Lonnie carbonatite complex, British Columbia. In: Geological Fieldwork 2013, British Columbia Ministry of Energy and Mines, British Columbia Geological Survey Paper 2014-1, pp. 169-182.

Abstract
The Lonnie carbonatite complex is the third most developed Nb prospect in the British Columbia alkaline province. The objective of this study was to determine the best size fraction of stream sediments for carbonatite related indicator mineral surveys. Sediments from seven sites along Granite Creek, a stream that transects the Lonnie deposit and adjacent bedrock units, were sampled for pXRF and pathfinder element studies. The results for key pathfinder elements including Nb, Ta, La, Ce, Pr, Nd, Y, P, Sr, Ba, Th, and U were precise (most having %RSD less than 5%) and prone to bias. Results for eight size fractions separated by laboratory sieves indicated a systematic distribution of key elements, with the highest abundances found in the finer size fractions. Of these, the +125µm fraction was chosen for further consideration due to its suitability for continued indicator mineral studies. With the exception of Ba, Sr, and possibly Nb samples upstream from the Lonnie deposit display higher concentrations of carbonatite pathfinder elements than samples downstream of the deposit. This indicates source(s) farther upstream, probably the Vergil carbonatite and Nb and TREE + Y soil geochemical anomalies. Indicator mineral studies are ongoing.

Keywords: Niobium, rare earth elements, carbonatite, indicator minerals, stream sediments, XRF

1. Introduction

Carbonatites, carbonatite-related alteration zones, and their weathered equivalents are the most important sources of Nb, and rare earth elements (Simandl et al., 2012). They contain important deposits of Ta, vermiculite, apatite (phosphate), badelleyite (zirconia), fluorite, U, and magnetite (Birket and Simandl, 1999, Mariano 1989a, 1989b). Although carbonatites are observed mainly in intracratonic rift settings, they are also present along cratonic margins (Woolley and Kjarsgaard, 2008), such as near the western flank of ancestral North America, in the British Columbia alkaline province (inset, Fig. 1).

One of the main objectives of the Specialty Metals component of the Targeted Geoscience Initiative 4 (TGI-4) is to determine if indicator minerals can guide explorationists toward carbonatite-related mineralization or at least toward carbonatites themselves. But processing heavy minerals and analysis of indicator minerals is relatively expensive and time consuming. Therefore, as an orientation survey, we measured the concentrations of Nb, Ta, REE, P, Sr, Ba, U, and Th in different grain size fractions of sediments sampled from streams draining three deposits. We used a portable X-ray fluorescence (pXRF) device to minimize the cost, improve output, and optimize the method (assuming that pyrochlore, columbite-tantalite, fersmite, apatite, REE-bearing fluorocarbonates, monazite, allanite, zircon, xenotime, and minerals of celestite-barite solid solution will be present in sediments downstream of the deposits).

Herein are results from Lonnie, a carbonatite-related Nb prospect, 7 km east of the Manson Creek settlement and 220 km northwest of Prince George (Fig. 1). Results from the Aley carbonatite, a large advanced Nb project, and the Wicheeda carbonatite plug, a medium-sized advanced rare earth element (REE) project (Fig. 1) will be presented elsewhere. We focus on grain size distributions and chemistry of samples collected near the Lonnie carbonatite; future work will concentrate on analysis of indicator minerals.

2. Geology of the Lonnie carbonatite

The Lonnie carbonatite complex belongs to a series of metacarbonatites, syenite complexes, and other alkaline rocks forming the British Columbia alkaline province (Fig. 1; Pell, 1994; Simandl et al., 2012). It is in the southern Omineca Mountains, which straddle the boundary between the Intermontane and Omineca belts. The Lonnie metacarbonatite outcrops along the projection of the Wolverine fault (Fig. 2), an extensional structure sub-parallel to the nearby dextral, 1-5 km wide Manson Creek fault system (Simandl et al., 2013a). The Wolverine fault is a probable metallotect connecting the Lonnie deposit to the Virgil carbonatite, 4.5 km to the northwest. This fault system is considered part of the Rocky Mountain Trench, separating the Quesnel terrane from the Slide Mountain and Cassiar terranes (Ferri and Melville, 1994).

Northwest of the Wolverine fault zone the Granite Creek drainage area is underlain by amphibolite-grade rocks of Ingenika Group (Neoproterozoic), and schists and quartzite of the Wolverine Metamorphic complex (Fig. 2). Bordering these

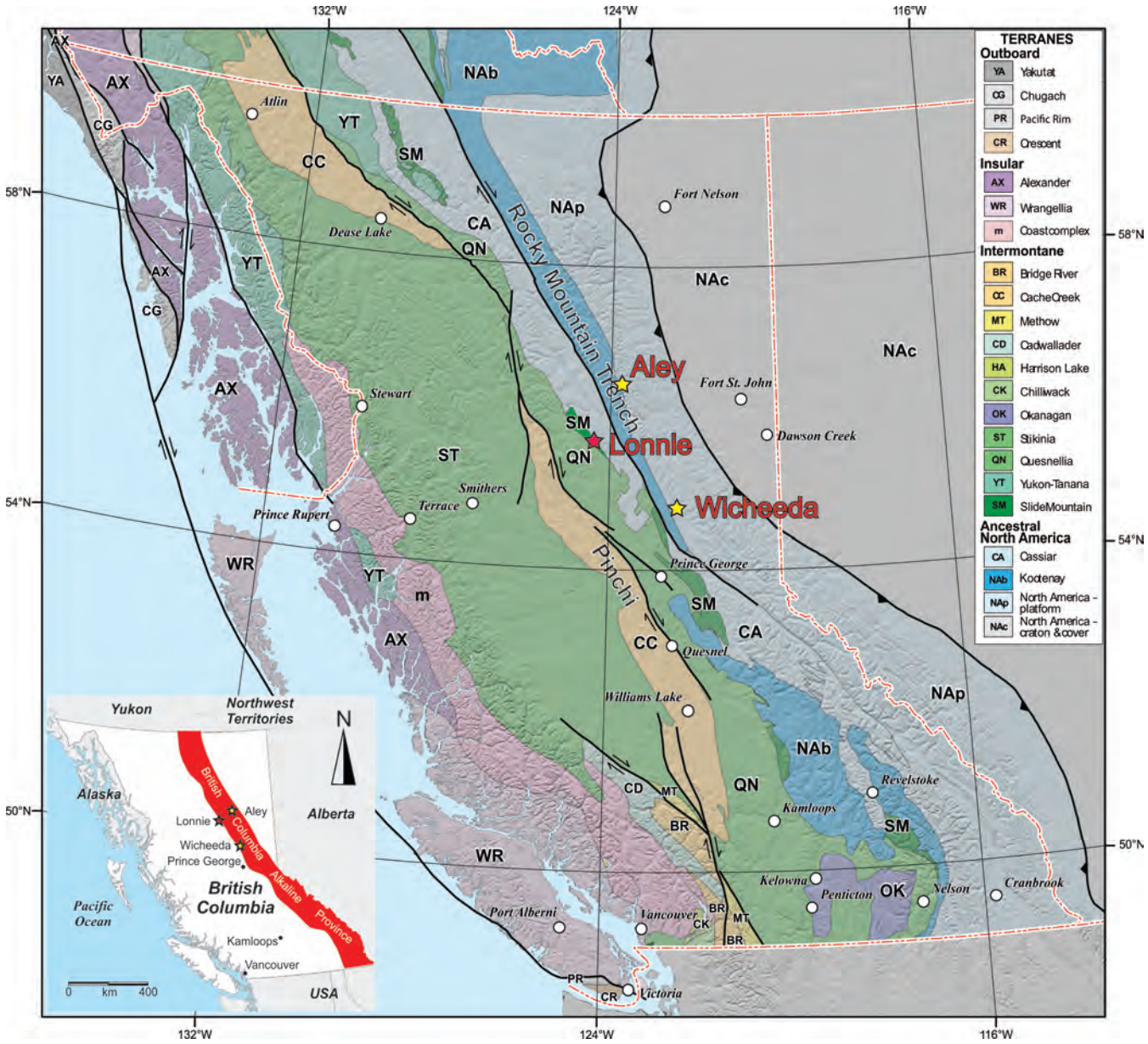

Fig. 1. Location and tectonic setting of the Lonnie carbonatite complex. Communities are indicated with white circles. Overview map modified from Colpron and Nelson (2011), inset from Pell (1994).

rocks along the hanging wall of the Wolverine fault zone is the Lonnie carbonatite complex. Farther southwest, siliciclastic and carbonate rocks of the Stelkuz Formation, limestone of the Epsee Formation, and metapelites of the Tsaydiz Formation comprise the Wolverine antiform (Ferri and Melville, 1994; Simandl et al., 2013a). Farther to the west are the Nina Creek and Big Creek groups (Fig. 2).

The Lonnie carbonatite complex has been explored episodically for sixty years (Thompson, 1955; Helmel, 2012; Simandl et al., 2013a). Traced by trenching over a length of 650 metres, it is up to 50 metres wide. Several Nb ± REE soil anomalies were identified near the deposit (Fig. 2; Helmel, 2012). The deposit consists of biotite-bearing sövite, aegerine-amphibole sövite, and a variety of quartz-free feldspathic rocks, probably produced by fenitization. Blue-green amphiboles and aegirine decrease away from the carbonatite in fenitized metasediments (Simandl et al., 2013a). A 1955 trenching program (pre- NI-43-101) reported a mineralized zone 530 metres long and approximately 17 metres wide grading 0.21% Nb_2O_5 (Rowe, 1958; Chisholm,1960). In this zone, the Na-amphibole-bearing carbonatite assayed 0.16% Nb_2O_5 over 6 metres. The feldspathic rocks averaged 0.23% Nb_2O_5 over nearly 10 metres. Furthermore, the central portion of this zone averaged 0.3% Nb_2O_5 across 8.3 metres over a length of 283 metres (Rowe, 1958). Recent analyses (Simandl et al., 2013a) failed to confirm these grades. Pyrochlore seems to be the main Nb-bearing mineral (Simandl et al., 2013a); however, columbite was also reported (Hankinson, 1958; Halleran, 1980;

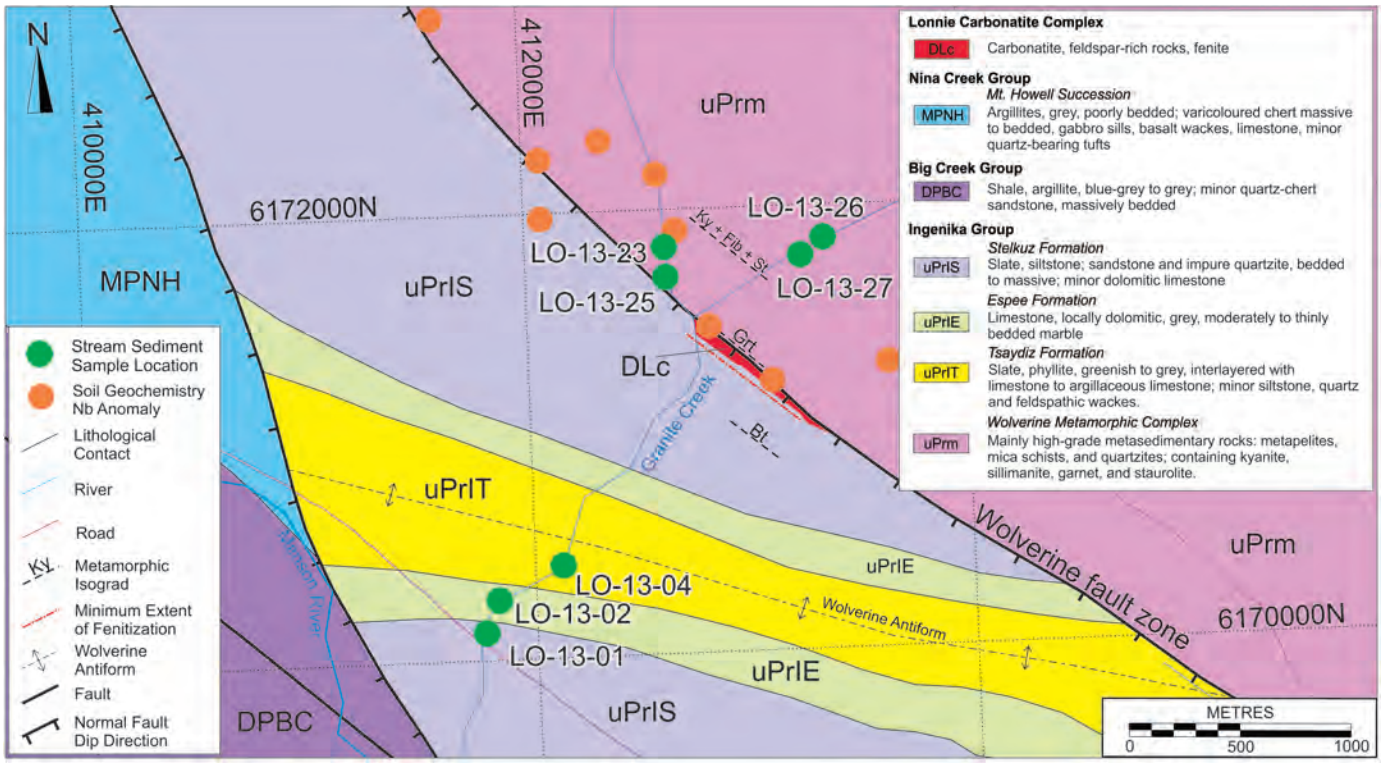

Fig. 2. Regional geologic map with sample locations. UTM coordinates are zone 10, North American Datum 1983.

Pell, 1994) and Nb-bearing rutile was reported in polished thin sections. Pell (1994) reported up to 20% apatite in the carbonatites and 3-15% zircon in associated nepheline syenite. Accessory ilmenite and ilmenorutile have also been reported (Hankinson, 1958).

3. Sampling procedure

Samples of stream sediment were collected along the drainage of Granite Creek (Fig. 2; Table 1), upstream and downstream of the Lonnie deposit. The location and spacing of samples was controlled by accessibility, as Granite Creek runs within a canyon. There is more than 180m elevation difference between sample LO-13-26 and LO-13-01. The bed of the stream consists mainly of boulders, cobbles, and pebbles. Most of the sample sites are in the lee of large boulders or logs where the material was deposited in the final stages of bedload transport. The fraction of sediments that passed through an 8 mm sieve was kept. Samples were contained in permeable canvas bags and stored in plastic pails.

4. Laboratory procedure

4.1. Sample preparation

Samples were processed at the British Columbia Geological Survey Laboratory in Victoria. Small samples were dried in a Despatch LBB Series oven (1600 Watts, 13.3A) for 24 hours at temperatures between 38 and 40°C, whereas large samples were dried for 48 hours. Separation of dry samples into eight size fractions was carried out using a Humboldt MFG. Co. laboratory sieve (serial number H4325-136). The following size fractions were separated: +4 mm, 2 mm to 4 mm, 1 mm to 2 mm, 500 µm to 1 mm, 250 µm to 500 µm, 125 µm to 250 µm, 63 µm to 125 µm, and -63 µm. For the most thorough separation of each size fraction the uppermost sieve compartment was filled no more than 3 cm from its bottom; shaking time was eight minutes. The procedure was repeated until each sample was completely sieved. Individual fractions were stored in Kraft® sample bags. Before processing a new sample, each sieve was scrubbed clean using a stiff brush and a Haver USC 200-80 ultrasonic bath.

Each size fraction passed through a riffle-type splitter. Part of the sample was kept as a witness; the remainder was further split for pXRF analyses and for magnetic separation using an isodynamic separator (Frantz). Milling was carried out with Rocklabs Limited tungsten carbide mills consisting of a ring and roller bowl for three minutes. Compressed air was used to clean the milling equipment. When required, silica sand was milled between individual samples. In all cases equipment was washed with water and dried using a combination of compressed air followed by drying in a Despatch oven at 40°C to drive off surface moisture.

Standard XRD sample cups covered by 4µm polypropylene film were filled with sediment pulp and compressed. Two filter papers (2.4 cm in diameter) were placed over the pulp, and the remainder of the sample cup was filled with gauze to ensure a snug fit when capped. To avoid contamination of the pXRF stage by pulp residue, the sides of the cup were wrapped in parafilm.

Table 1. Descriptions of stream sediment sample sites in the Granite Creek drainage (July 2013).

	Location (UTM Zone 10, NAD83)		Elevation	Stream Characteristics					
Sample	Northing	Easting	(m)	Width (m)	Depth (m)	Flow	Clast Characteristics	Weight (g)	Sample Site
LO-13-01	6170135	411788	912	5	0.5	rapid	Rounded granite gneiss boulders < 1.5 m; average 8-15 cm.	16093.3	Lee of a log. Sand (< 2 mm); quartz, feldspar, biotite, white mica, sericite schist, and trace garnet. Not sieved in the field. Upstream from bridge.
LO-13-02	6170253	411895	915	4	0.75	rapid	Rounded granite gneiss and rare angular schist boulders < 2 m, average 2-10 cm.	5369.1	Lee of 1-2 m boulders. Sand (< 2 mm); sericite schist fragments, quartz, feldspar, biotite, opaques, and white mica particles. East side of stream flanked by 50 m cliff.
LO-13-04	6170326	412085	929	6	0.5	very rapid	Rounded granite gneiss and white mica granite boulders 40 cm-1.5 m.	8540.5	Lee of a boulder. Cobbles (5-15 cm) with sand (1-2 mm) forming matrix. Upstream from major slide. Trees right to the bank.
LO-13-23	6171607	412690	1030	4	0.5	rapid	Gneiss, muscovite schist, and quartzite < 1.5 m; average 5-15 cm	8323.2	Lee of boulders adjacent to submerged outcrop 5 m below rapids. Inside of a bend. Coarse sand and granules (2-3 mm) of quartz, feldspar, and mica form matrix. Minor free garnet; approximately 0.5 mm, rounded, Cliffs flank east side of creek.
LO-13-25	6171598	412797	1032	-	-	-	Gneiss, muscovite schist, and quartzite < 1.5 m; average 5-15 cm	3711.6	Narrow levee 2 m from stream edge. Quartz sand coarsening toward the stream. Similar to LO-13-23.
LO-13-26	6171813	413331	1095	3	0.5	rapid	Gneiss and schist 5-15 cm	3833.2	Lee of boulders under a log. Sand (average 2 mm) slate fragments, rare deep red and rose garnet, apatite, pyrite. 4 m downstream from rapids, upstream from road crossing.
LO-13-27	6171813	413331	1095	3	0.5	rapid	Gneiss and schist 5-15 cm	4856.9	Lee (0.5 x 2m) of large log. Sand (2 mm average) fining upward. Similar to LO-13-26.

4.2. Portable x-ray fluorescence

Analyses were carried out using a portable Thermo Fisher Scientific Niton FXL-950 instrument (Fig. 3; manufactured on July 17, 2012). This model is equipped with an Ag anode x-ray tube (serial number 56789-00109) capable of a maximum voltage of 50 kV, current of 0.2 mA, and power of 4 W. Four beams were used to detect elements (Table 2). Analytical time of each beam was set at 60 seconds with a spot size of 8mm. The "mining Hf/Ta mode" was chosen to obtain the highest resolution measurements of fluorescent peaks for high field strength elements (HFSE), which are of interest for the investigation of Nb and REE deposits.

Detection limits for Nb, Ta, La, Ce, Pr, Nd, Y, Ba, Sr, and P are given in Table 3. The pXRF methodology in this study

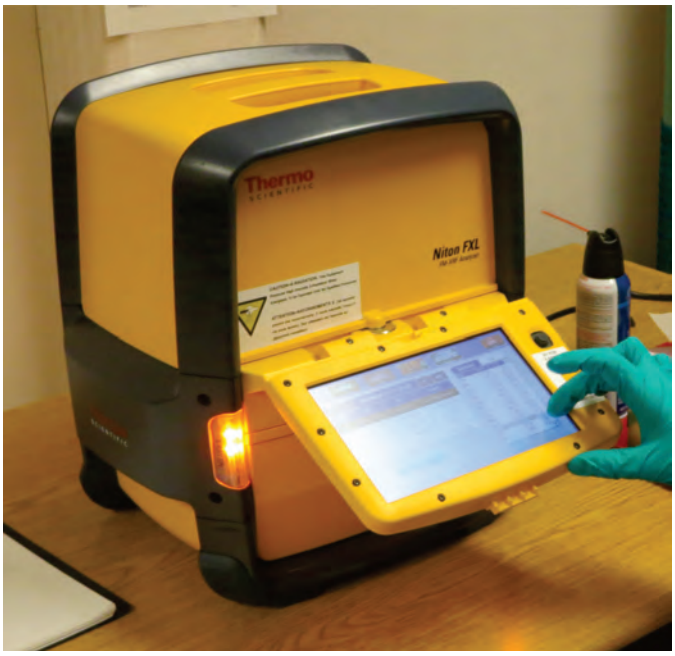

Fig. 3. The pXRF Thermo Fisher Scientific Niton FXL-950 instrument used in this study.

is described in Simandl et al. (2013c). At the start of each session, the pXRF was allowed 10 minutes to achieve a stable temperature (approximately - 25°C) before running a system check. Analyses of five standard reference materials bracketed stream sediment samples. These standards included a 99.995% SiO_2 blank, Standard Reference Material NIST 2780 (May and Rumble, 2004), Certified Reference Material "TRLK" Rare Earth Ore "CGL 124" (Registration Number: USZ 42-2006; Mongolia Central Geological Laboratory, 2006), and Reference Niobium Ore OKA-1 (Steger and Bowman, 1981). Samples were subjected to three repeat analyses to measure precision and ensure homogeneity.

5. Data quality

The accuracy and precision of the pXRF data can be assessed by considering the results of repeated analyses on standard reference materials of known composition (Tables 4, 5, and 6). Accuracy is evaluated by percent difference:

$$\%\text{diff} = \frac{\text{measured value} - \text{reference value}}{\text{reference value}} \times 100\%$$

Precision was assessed as relative standard deviation expressed in percent (%RSD) and as defined by:

$$\%\text{RSD} = \frac{\text{standard deviation}}{\text{mean}} \times 100\%$$

Error bars on diagrams for results herein reflect the precision (2σ) established by multiple analyses of standards. Of the elements for which abundances are reported here, only Ce had results above the detection limit on blank analyses. For n=38 an average of 119 ± 28 (2 σ) Ce was detected. For this reason, results for Ce should be considered higher than true values.

Analyses of the standard reference material NIST 2780 (Table 4) resulted in %diff less than 10% for Ca, Sr, Th, and Zr; less than 20% diff for Fe, Ti, and Ba; and 50% diff for S. Uranium, La, and Ce were over 100% diff and Nd was over 1000% diff. Certified values for NIST 2780 to compare with elemental abundances determined in this work for Ta, Y, and Pr are unavailable. The %RSD of Fe, Ca, Ti, Ba, S, Sr, Zr, and Y were less than 5%; Ce, Nd, and Pr were less than 10%. Thorium, U, and La had %RSDs of 26.4, 29.7, and 12.5%, respectively. No measurements above detection limits were made on P, Nb, or Ta.

Repeated determinations of elemental abundances by pXRF on the Mongolian rare earth ore TRLK CGL 124 resulted in %diff of 10% or less for Sr, La, Ce, Nd, and Pr (Table 5). For the elements Fe, Ca, Th, U, Nb, Zr, and Y it was between 10 and 46%, for Ba and S it was 160 and 170%. No determination of accuracy could be made for Ta, as certified values are unavailable. The precision was better than 5 %RSD for Fe, Ca, Ba, S, Sr, Th, Y, La, Ce, Nd, and Pr and better than 10% for U. Niobium, Ta, and Zr had %RSD of 11.8, 23.9, and 13.3% respectively.

The Nb Ore OKA-1 was evaluated for accuracy with reference to the CANMET certified values. For elements where no such value was available (indicated in Table 6) the average of three Li-borate fusion ICP-MS analyses carried out by ASL Limited (Vancouver) were used instead. The %diff of Fe, Ba, Sr, Nb, and Zr were less than 10%. Those of Ca, Ti, S, Y, La, and Ce, were less than 25%. For P, Th, U, Nd, and Pr the %diff ranged from 49 to 270%. The %RSD of Fe, Ca, P, Ti, Ba, S, Sr, Nb, Y, La, Ce, Nd, and Pr were less than 5%. Thorium, U, and Zr, had %RSDs of 23.8, 16.1, and 15.4.

Table 2. Elements and analytic time interval assigned to each of the four filters used in this study. [a] Represents the balance of fluorescence not attributed to any element analyzed here.

Beam	Duration (s)	Elements Analyzed
Main	60	Sb, Sn, Cd, Ag, Bal[a], Mo, Nb, Th, Zr, Y, Sr, U, Rb, Bi, As, Se, Au, Pb, W, Zn, Cu, Re, Ta, Hf, Ni, Co, Fe, Mn
Low	60	Cr, V, Ti, Ca, K
High	60	Nd, Pr, Ce, La, Ba, Sb, Sn, Cd, Ag
Light	60	Cl, S, P, Si, Al, Mg

Table 3. Detection limits for elements pertinent to carbonatite exploration. [a] Detection limits derived from a Thermo Fisher Scientific Niton XL3t Ultra; Thermo Fisher Scientific Niton FXL-950 is expected to have lower limits.

Element	Matrix	
	SiO_2 (ppm)	Natural sample or SiO_2+Fe+Ca (ppm)
Nb	2	2
Ta	NA	NA
Y[a]	1.5	4
La[a]	34	43
Ce[a]	40	47
Pr[a]	46	57
Nd[a]	75	93
Ba	28	33
Sr	2	2
P	80	90
U	NA	NA
Th	NA	NA
S	50	60

6. Results

Three samples (LO-13-04, LO-13-23 and LO-13-26) were selected for detailed study to identify grain size fractions that have the best potential to carry carbonatite indicator minerals (Fig. 4). Sample LO-13-04, not sieved through an 8mm screen in the field, consists mainly of grains coarser than +250 µm (medium sand). Sample LO-13-23 displays a positively skewed grain-size distribution. LO-13-26 contains subequal +2 mm, +1 mm, +500 µm, and +250 µm populations.

Niobium, Y, La, Ce, U, and Th are relatively enriched in the +125 µm, +63 µm, -63 µm size fractions (Fig. 4, Table 7). Barium, Sr, Pr, Nd, and Ta show less consistent patterns, nevertheless they are always detectable. Phosphorus is consistently detectable only in the +125µm fraction. Based on this information, similar findings from Aley carbonatite and Wicheeda drainages (Mackay and Simandl 2014a; 2014b), and because of other work (McClenaghan, 2011) indicating that the +250 µm, +125 µm, +63 µm fractions can be effectively used for indicator mineral studies, the +125 µm fraction was chosen for systematic study.

The +125 µm fraction of each of the seven samples collected in the Lonnie area was analysed for major and selected trace elements using pXRF. The ranges in abundance for major oxides are: 65.1 - 71.0 wt% SiO_2, 6.8 - 7.9 wt% Al_2O_3, 2.63-5.93 Fe_2O_3, 1.06-2.47 CaO, 0.28-1.59 TiO_2, 0.3- 0.5 wt% MgO,

Table 4. Results of repeated analyses on the NIST Standard Reference Material 2780. The number of readings above the detection limit is denoted as "n", standard deviation (1σ) as Std Dev. See text for details of %diff and %RSD. [a] Non-certified values supplied by Thermo Scientific.

		Certified values			pXRF values			
		ppm	+/-	n	Average	Std Dev	%diff	%RSD
Major Elements	Fe	27800	800	38	31400	345	13	1.1
	Ca	1950	200	38	1870	82	4	4.4
	P[a]	427	40	-	-	-	-	-
	Ti[a]	6990	190	38	6200	249	11	4.0
	Ba[a]	993	71	38	840	16	15	1.9
	S	12600	420	38	18800	327	50	1.7
Trace Elements	Sr[a]	217	18	38	232	4	7	1.5
	Th	12	-	38	13	3	7	26.4
	U	4	-	26	13	4	227	29.7
Specialty Metals	Nb	18	-	-	-	-	-	-
	Ta	-	-	-	-	-	-	-
	Zr	176	-	38	193	2	9	1.1
REE	Y	-	-	38	168	3	-	1.8
	La	38	-	38	90	12	156	12.5
	Ce	64	-	38	180	15	176	8.6
	Nd	28	-	38	330	29	1064	8.9
	Pr	-	-	38	180	13	-	7.2

Table 5. Results of repeated analyses on the Certified Reference Material "TRLK" rare earth ore CGL 124. The number of readings above the detection limit is denoted as "n", standard deviation (1σ) as Std Dev. See text for details of %diff and %RSD. [a] Converted to ppm from the oxide weight percent reported by the Mongolia Central Geological Laboratory.

		Certified Values			pXRF Values			
		ppm	+/-	n	Average	Std Dev	%diff	%RSD
Major Elements	Fe[a]	39938.36	594.53	38	45400	588	14	1.3
	Ca[a]	233562.6	2858.78	38	259000	1103	11	0.4
	P[a]	688.24	15.64	-	-	-	-	-
	Ti[a]	1198.7	71.92	-	-	-	-	-
	Ba	307	10	38	800	23	160	2.9
	S[a]	560.65	-	38	1510	62	170	4.1
Trace Elements	Sr	4900	400	38	4450	40	9	0.9
	Th	946	51	38	1180	19	25	1.6
	U	51.4	-	38	75	4	46	5.6
Specialty Metals	Nb	31	4.54	38	23	3	27	11.8
	Ta	-	-	30	60	13	-	23.9
	Zr	136	-	38	80	11	40	13.3
REE	Y	167	20	38	209	2	25	1.1
	La	21100	1100	38	20700	169	2	0.8
	Ce	27600	500	38	27400	234	1	0.9
	Nd	6500	300	38	5900	150	10	2.6
	Pr	2300	300	38	2160	41	6	1.9

Table 6. Statistical assessment of repeated analyses of reference material OKA-1. The number of readings above the detection limit is denoted as "n", standard deviation (1σ) as Std Dev. See text for details of %diff and %RSD. Unless otherwise noted, values are from Steger and Bowman (1981). [a] Average of three analyses by Li borate fusion inductively coupled plasma mass spectrometry (LB-ICP-MS). The error bracket corresponds to the absolute difference of the most extreme outlier from the average.

		Certified or Laboratory Values			pXRF Values			
		ppm	+/-	n	Average	Std Dev	%diff	%RSD
Major Elements	Fe	28000	-	37	30600	494	9	1.6
	Ca	313000	-	37	354000	1592	13	0.4
	P	11000	-	37	4300	203	60	4.6
	Ti[a]	1358	40	2	1530	41	13	2.7
	Ba[a]	2887	117	37	3070	32	6	1.0
	S	6000	-	37	4900	157	18	3.2
Trace Elements	Sr[a]	13501	56	37	12400	63	8	0.5
	Th[a]	57	4	37	150	37	169	23.8
	U[a]	29	5	37	43	7	49	16.1
Specialty Metals	Nb	3700	0.01	37	3390	64	8	1.9
	Ta[a]	36	8	-	-	-	-	-
	Zr[a]	112	5	37	120	18	6	15.4
REE	Y[a]	61	1	37	74	2	20	2.4
	La[a]	1107	43	37	1360	20	23	1.4
	Ce[a]	2045	75	37	2310	32	13	1.4
	Nd[a]	535	13	37	1400	39	162	2.7
	Pr[a]	182	4	37	670	32	270	4.8

Table 7. Results of pXRF analyses in eight size fractions for LO-13-04, LO-13-23, and LO-13-26 and the +125µm size fraction for all other samples taken from the Lonnie study area. [a] Total iron is reported as Fe_2O_3.

Unit	Size Fraction	Nb ppm	Ta ppm	Y ppm	La ppm	Ce ppm	Pr ppm	Nd ppm	Ba ppm	Sr ppm	P ppm	U ppm	Th ppm	Fe_2O_3[a] wt%	CaO wt%	TiO_2 wt%	S ppm	Zr ppm
LO-13-04	+4mm	13	36	19	122	187	231	407	406	267	<90	<4	8	4.90	5.95	0.51	1616	126
	+2mm	14	48	13	81	136	145	251	425	201	<90	<4	8	3.90	2.11	0.34	<60	135
	+1mm	24	38	12	69	136	121	212	395	154	<90	<4	8	3.41	1.15	0.30	<60	129
	+500µm	18	51	11	57	102	99	177	309	134	<90	<4	6	2.59	0.91	0.24	<60	120
	+250µm	44	48	16	65	109	84	150	255	145	<90	<4	7	2.63	1.06	0.28	<60	131
	+125µm	72	38	36	134	208	131	225	294	181	155	4	22	3.38	1.51	0.50	<60	191
	+63µm	79	47	68	182	308	128	242	341	211	508	11	51	3.86	1.76	0.61	136	458
	-63µm	71	33	67	138	231	92	169	416	247	<90	12	36	5.57	1.81	0.56	<60	665
LO-13-23	+4mm	32	49	16	65	104	108	202	408	151	<90	<4	10	2.97	1.70	0.27	<60	95
	+2mm	14	51	14	43	79	61	91	297	136	<90	<4	8	2.96	1.19	0.25	<60	104
	+1mm	9	45	15	79	128	93	181	318	127	<90	<4	6	2.30	0.92	0.19	<60	87
	+500µm	29	34	27	49	88	78	150	256	112	<90	5	8	2.57	0.91	0.16	<60	105
	+250µm	54	48	57	76	133	89	168	227	121	123	6	26	3.40	1.27	0.25	<60	161
	+125µm	61	48	110	138	243	101	223	258	155	734	15	85	3.87	1.84	0.56	<60	283
	+63µm	61	50	131	246	434	125	269	339	188	<90	27	134	3.47	2.09	0.67	<60	715
	-63µm	57	37	125	188	338	64	158	409	200	<90	27	94	4.84	1.83	0.65	<60	1213
LO-13-26	+4mm	8	44	15	83	137	143	265	285	119	<90	<4	<5	3.65	1.51	0.30	<60	111
	+2mm	12	47	17	65	117	127	227	266	116	<90	<4	5	3.53	1.36	0.31	<60	101
	+1mm	8	47	21	69	114	117	221	252	113	<90	<4	7	3.18	1.10	0.24	<60	97
	+500µm	19	36	23	64	102	107	166	213	102	<90	<4	6	2.71	0.95	0.20	<60	106
	+250µm	32	48	52	95	171	177	324	210	119	<90	<4	9	3.74	1.35	0.33	<60	133
	+125µm	75	62	118	193	353	232	478	228	163	660	15	56	5.95	2.27	1.09	<60	376
	+63µm	103	49	212	436	768	228	537	277	187	<90	47	178	5.38	2.47	1.59	<60	1660
	-63µm	42	32	113	242	401	103	235	360	205	<90	27	78	5.34	1.80	0.66	<60	1224
LO-13-01	+125µm	51	47	27	103	172	122	217	280	182	141	4	14	2.68	1.57	0.46	<60	157
LO-13-02	+125µm	73	38	33	135	217	142	274	297	178	178	7	19	3.26	1.54	0.51	<60	192
LO-13-25	+125µm	39	41	67	123	216	143	240	244	156	407	8	46	2.84	1.64	0.42	<60	228
LO-13-27	+125µm	16	50	23	57	107	111	195	219	151	<90	<4	10	2.61	1.48	0.31	<60	120

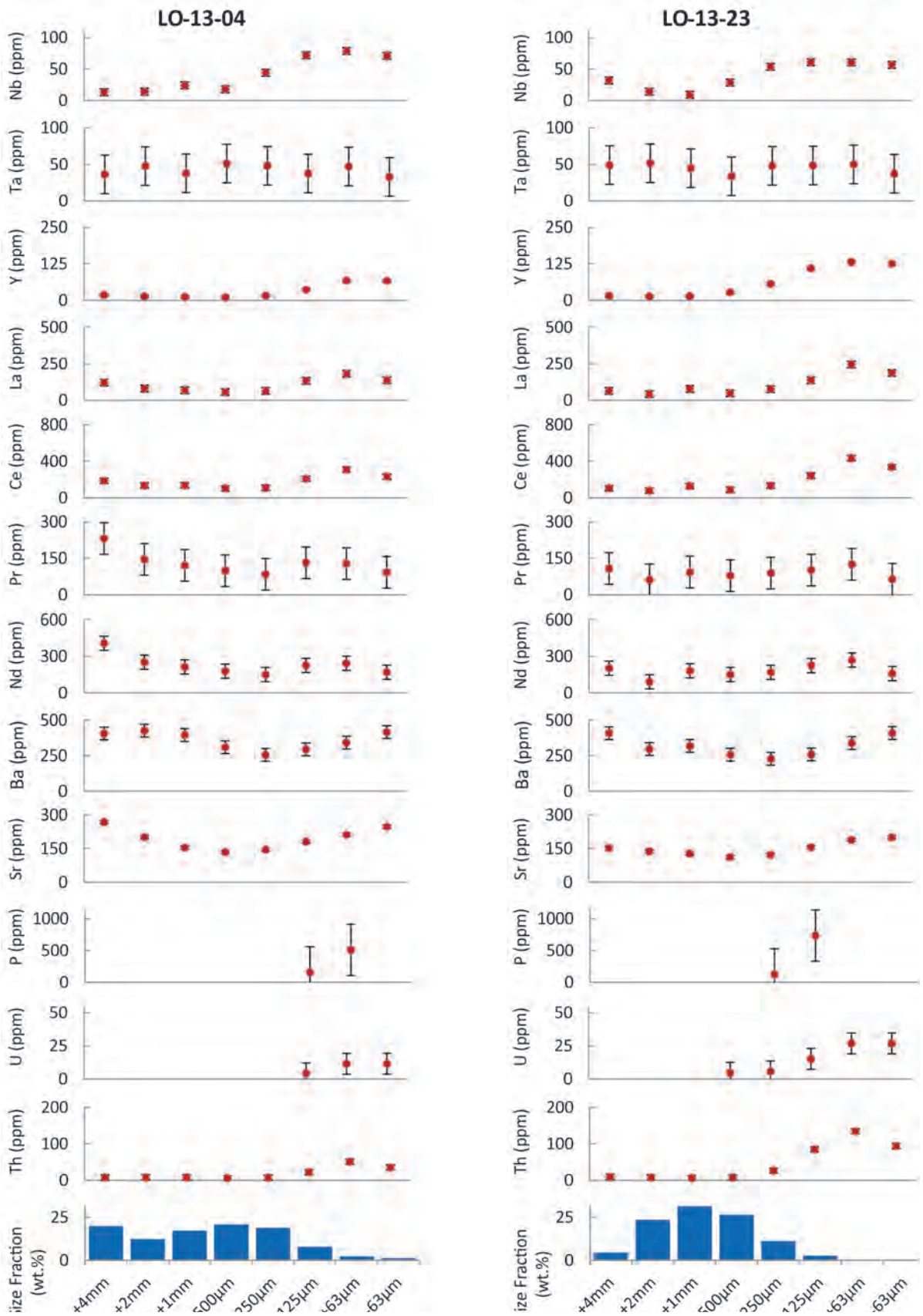

Fig. 4. Concentrations of elements, as determined by pXRF, that are expected to coincide with the greatest concentrations of indicator mineral grains for eight grain size fractions in samples LO-13-04, LO-13-23 and LO-13-26.

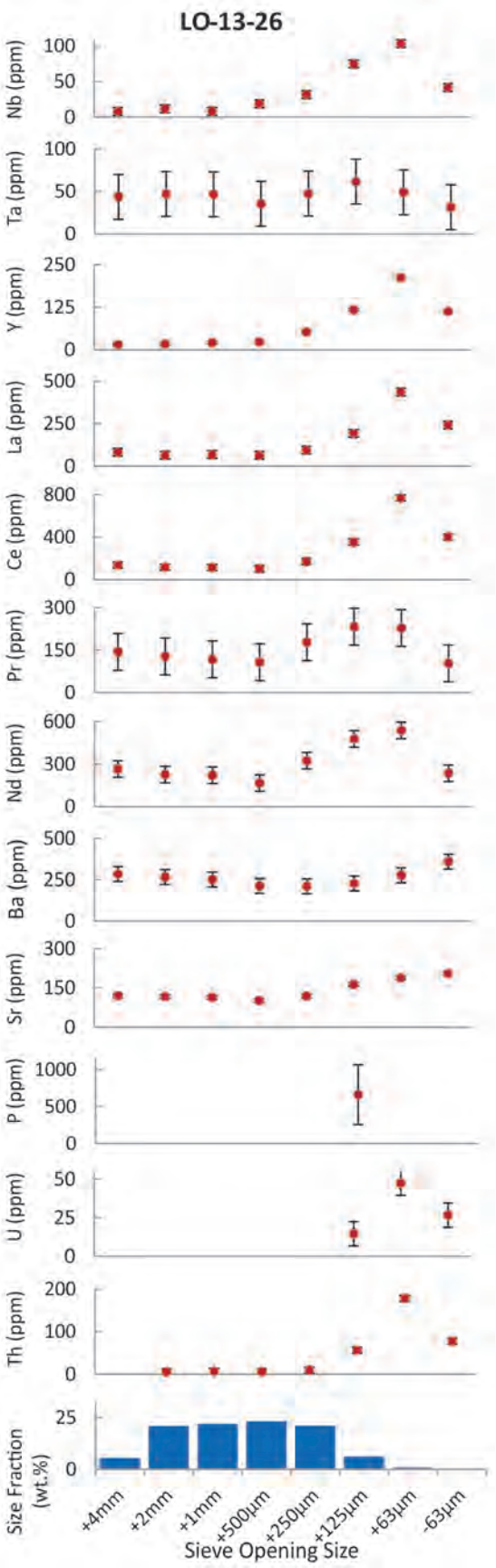

Fig. 4. Cont'd.

1.1 to 1.4 wt% K_2O and < 60-136 ppm S (Table 7).

Linear dependence between target elements and with other major and trace elements are common in sediments collected from Granite Creek (Fig. 5). There is a moderate correlation between Nb and La ($R^2 = 0.72$), a poor correlation between Nb and TiO_2 ($R^2 = 0.41$) or Fe_2O_3 ($R^2 = 0.38$); Nb and Ta do not correlate ($R^2 = 0.002$). Cerium correlates well with La ($R^2 = 0.96$). Correlations between Ce and Nd ($R^2 = 0.77$), Ce and Pr ($R^2 = 0.64$) and Ce and Y ($R^2 = 0.69$) are weaker. For P, correlations are strongest with Y ($R^2 = 0.97$), Th ($R^2 = 0.92$), and U ($R^2 = 0.93$), becoming progressively weaker with Ce ($R^2 = 0.53$), La ($R^2 = 0.38$), and Nd ($R^2 = 0.21$). Zirconium correlates strongly with Ce ($R^2 = 0.92$), Y ($R^2 = 0.89$), and U ($R^2 = 0.80$), and to lesser extend with Nd ($R^2 = 0.68$) or Pr ($R^2 = 0.53$). Significant linear dependencies also exist for Ca-Zr ($R^2 = 0.91$), Ca-Ce ($R^2 = 0.81$), Ca-Nd ($R^2 = 0.78$), Ca-U ($R^2 = 0.70$), Ca-P ($R^2 = 0.66$), Ca-La ($R^2 = 0.64$) and Ca-Pr ($R^2 = 0.60$). Also of interest are the correlations of Fe_2O_3 with TiO_2 ($R^2 = 0.96$), Th with U ($R^2 = 0.82$), and Sr with Ba ($R^2 = 0.74$).

7. Discussion

Statistical assessments of pXRF results for standard reference materials (Tables 4, 5, and 6) indicate that the method is precise but prone to bias. Elements with the highest accuracy (less than 30%diff) in concentration ranges observed at Lonnie are Nb, Y, Sr, Th, Fe_2O_3, CaO, and TiO_2. Lanthanum, Ce, Nd, Ba, and U have %diff exceeding 100%. The % diff values for Ta, Pr, and P are unavailable.

Recommended values for standard reference materials are reported as a mean of results from several different techniques, making comparison with results from pXRF complicated. From a practical point of view pXRF analyses presented in this paper should be viewed as internally consistent but relative. Recalibration using results of standard laboratory analyses (as described in Simandl et al., 2013b) to correct for matrix effects and analytical biases to improve accuracy has not been performed.

Sediment size fractions commonly examined and hand picked for indicator minerals include 0.25-0.5 mm, 0.3-0.5 mm, and 0.25-0.86 mm (McClenaghan, 2011). The three finest size fractions from this study, +125 µm, +63 µm, and -63 µm, have the highest abundances of all potential pathfinder elements (Fig. 4). The +125 µm is the only size fraction that consistently returned results above the 90 ppm detection limit for P, a constituent of apatite, monazite, and xenotime, which are indicator minerals in REE exploration. The +125 µm size fraction is also the coarsest fraction of those enriched in carbonatite pathfinder elements, making it potentially the most versatile from the explorationist's point of view. However, both the +125 µm and +63 µm size fractions will be the subject of quantitative evaluation of minerals by scanning electron microscopy (QEMSCAN®)-based indicator mineral studies that we are initiating in collaboration with ACME Labs™.

Both geochemical and indicator mineral surveys relying on stream sediment sampling are based on the premise that the

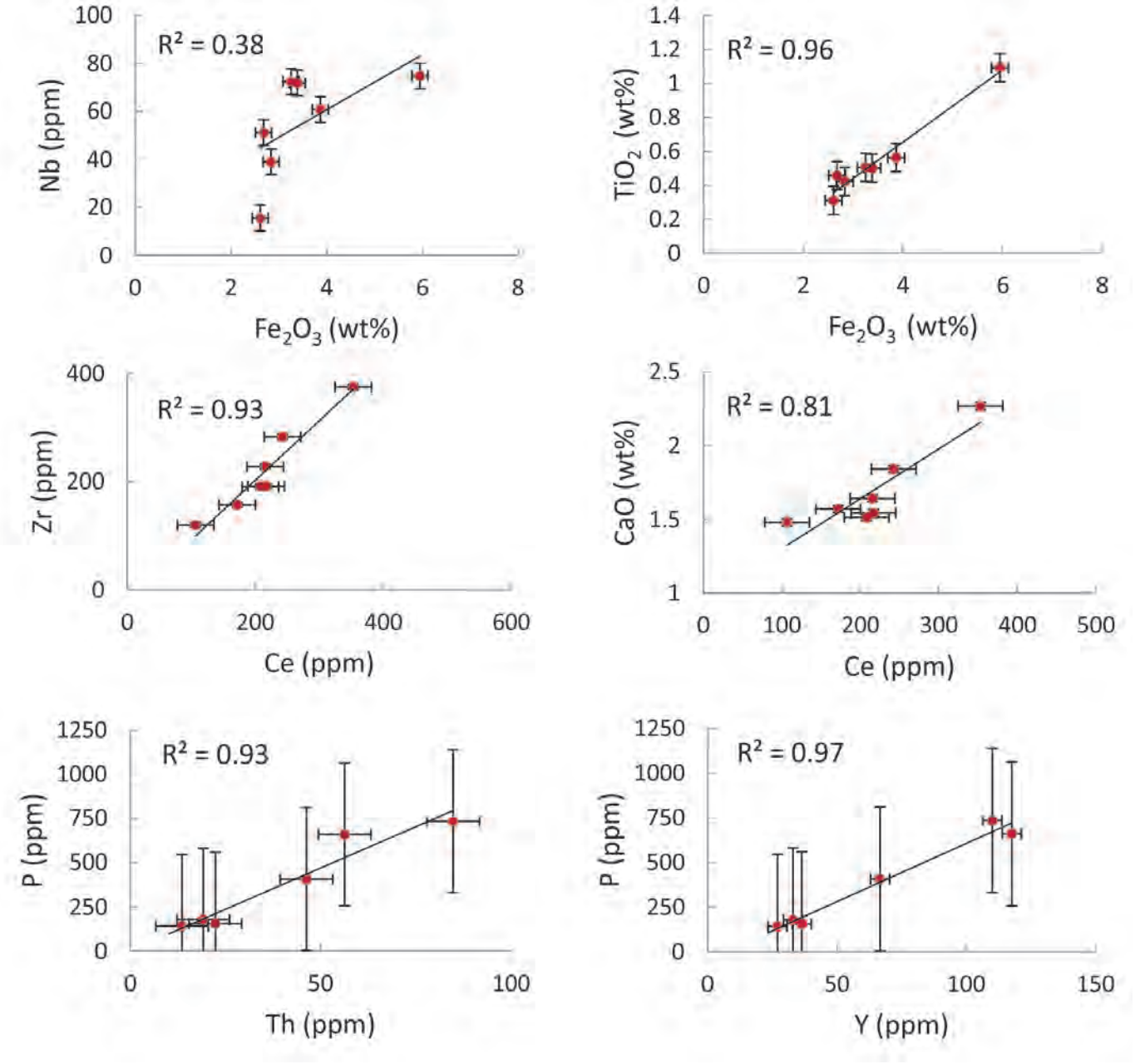

Fig. 5. Linear interpolation of elemental abundances analyzed by pXRF. The R^2 indicates strength of correlation with R^2=1 for totally dependent and R^2=0 for no relationship.

stream sediment sample is representative of the sample site. Assuming derivation of pathfinder elements and minerals from a single deposit (point source; Lonnie carbonatite), Hawkes' (1976) model should apply. Under such conditions, enrichment in carbonatite pathfinder elements (Nb, Ta, La, Ce, Pr, Nd, Y, Ba, Sr, P, U, and Th) immediately downstream of the point source relative to background abundances upstream of the point source is expected. A measurable decrease in pathfinder element abundances with increasing distance downstream of the point source is also expected until background abundances are reached.

Concentrations of pathfinder elements in stream sediments sampled in the vicinity of the Lonnie carbonatite complex are not in agreement with the ideal distribution of Hawkes' (1976) model. The upstream samples (LO-13-23, LO-13-25, LO-13-26, LO-13-27; Fig. 6) were taken to establish background concentrations of carbonatite indicator elements. No clear enrichment in Nb, Ta, La, Ce, Pr, Nd, Y, P, U, and Th in samples downstream of the Lonnie deposit (LO-13-01, LO-13-02, LO-13-04) was observed relative to those upstream of the deposit; only Ba and Sr concentrations are higher downstream of the deposit (Fig. 6; Table 7). The highest concentrations of Ta, La, Ce, Y, P, U, and Th were in samples upstream of the Lonnie carbonatite complex (LO-13-23 and LO-13-26; Fig.

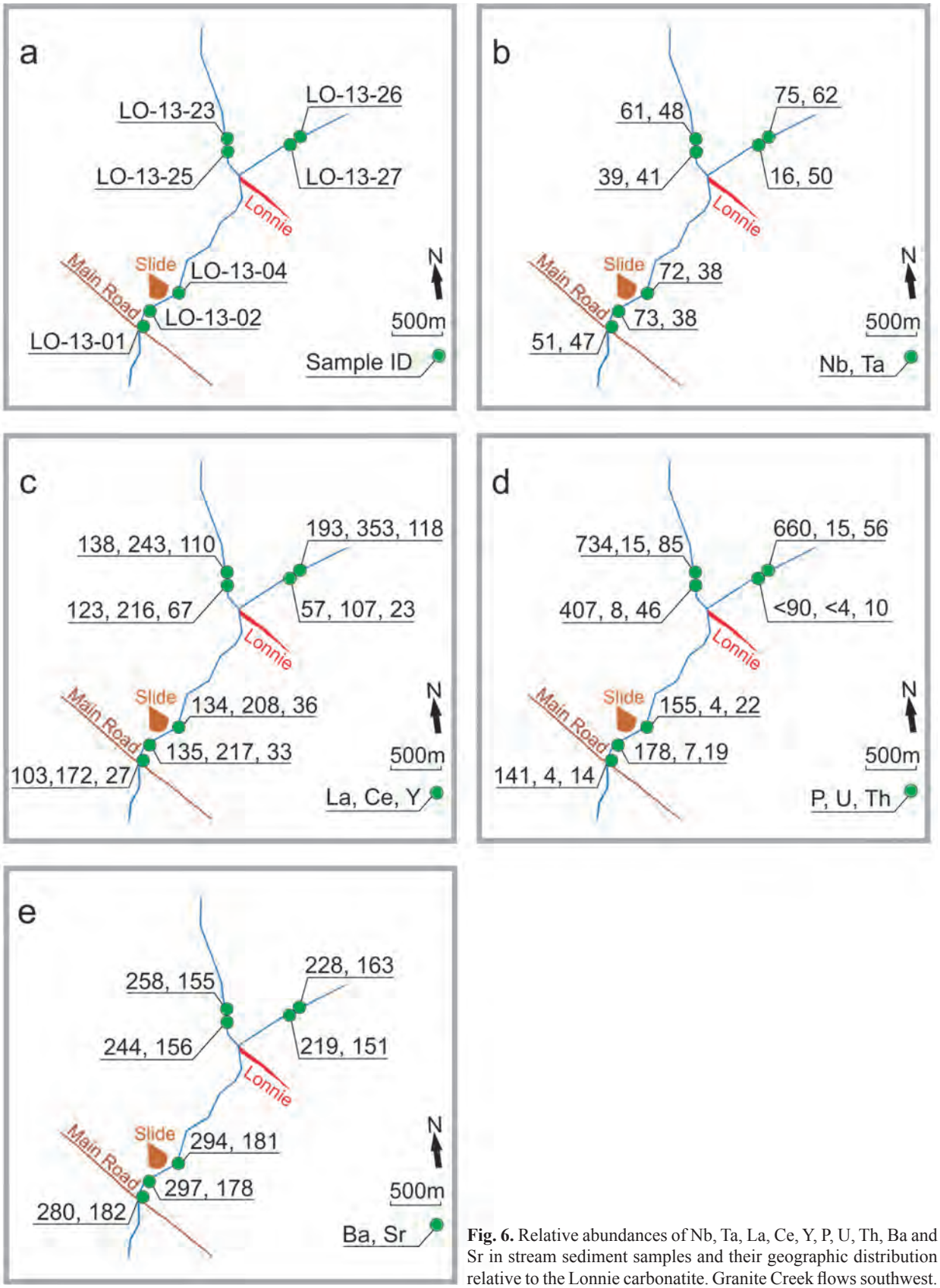

Fig. 6. Relative abundances of Nb, Ta, La, Ce, Y, P, U, Th, Ba and Sr in stream sediment samples and their geographic distribution relative to the Lonnie carbonatite. Granite Creek flows southwest.

6), suggesting that their main source is farther upstream. The most likely sources are the Vergil carbonatite (4.5 km to the northwest) and a number of Nb and TREE + Y soil geochemical anomalies (Fig. 2) identified by Rara Terra Minerals Corp. and reported by Helmel (2012).

It is unclear whether or not the Lonnie carbonatite complex is detectable by bulk stream sediment chemistry. Uncertainty is largely due to the lack of samples over a distance of more than 1300m between the Lonnie deposit and the nearest downstream sample (LO-13-04). All three of the samples downstream of the Lonnie carbonatite complex (LO-13-01, LO-13-02, and LO-13-04) are situated in a canyon. Dilution by mass wasting may have masked the influence of the Lonnie carbonatite complex on pathfinder element concentrations in these samples.

The relationships between potential indicator elements shown on X-Y plots (Fig. 5) reflect the relative proportions of indicator minerals in the sample and the chemical composition of these minerals. Frantz isodynamic separator can be used to amplify the pathfinder elements signal to noise ratio. The lack of correlation between Nb and Ta can be explained by poor pXRF precision for Ta (Table 5). Phosphorus correlations with Th and the REE may indicate the presence of monazite. Although none has been observed at Lonnie, monazite may be in the Wolverine Metamorphic complex. These elements also correlate strongly with Zr, where their relatively high abundances suggest co-occurrence of a REE-bearing mineral with zircon rather than REE being exclusively entrained within its matrix. The correlations of REE with calcium may be explained by substitution in apatite, monazite, or fluorocarbonates.

8. Conclusion

This study shows that the +125 μm size fraction is most appropriate for consideration in carbonatite indicator studies. Portable XRF is an excellent tool to assess relative abundances of elements to determine the most appropriate size fraction for indictor mineral sampling. However, a calibration procedure as described by Fajber and Simandl (2012) and Simandl et al. (2013b) should be used if increased accuracy is required. Irregular sample distribution downstream of the Lonnie deposit prevents us from concluding if the carbonatite is detectable using bulk stream sediment chemistry. Available data suggests that the main source of pathfinder elements, with the exception of Ba and Sr, is located upstream of the Lonnie carbonatite complex, possibly Vergil carbonatite or sources of Nb and TREE + Y anomalies identified by Rara Terra Minerals Corp. Much of the uncertainty in this data set will be clarified following the processing of samples by Frantz isodynamic separation and study of indicator minerals in resultant concentrates.

Acknowledgments

We thank Duncan Mackay for his assistance in the field. This project received funding and support from Targeted Geoscience Initiative 4 (2010-2015), a Natural Resources Canada program carried out under the auspices of the Geological Survey of Canada. Review and suggestions for improvement by Ray Lett and Duncan Mackay of the British Columbia Geological Survey are much appreciated.

References cited

Birkett, T.C. and Simandl, G.J., 1999. Carbonatite associated deposits. In: Simandl, G.J., Hora, Z.D., and Lefebure, D.V. (Eds.), Selected British Columbia Mineral Deposit Profiles, Vol. 3: Industrial Minerals and Gemstones. British Columbia Ministry of Energy, Mines and Petroleum Resources, British Columbia Geological Survey, Open File 1999-10.

Chisholm, E.O., 1960. Lonnie columbian deposit. British Columbia Ministry of Energy and Mines property file <http://propertyfile.gov.bc.ca/showDocument.aspx?&docid=138373> accessed October 2013.

Colpron, M. and Nelson, J.L., 2011. A digital atlas of terranes for the northern Cordillera. British Columbia Ministry of Energy and Mines, British Columbia Geological Survey, GeoFile 2011-11.

Fajber, R., and Simandl, G.J., 2012. Evaluation of Rare Earth Element-enriched Sedimentary Phosphate Deposits Using Portable X-ray Fluorescence (XRF) Instruments. In: Geological Fieldwork 2011, British Columbia Ministry of Energy, Mines and Natural Gas, British Columbia Geological Survey Paper 2012-1, pp. 199-209.

Ferri, F. and Melville, D.M., 1994. Bedrock geology of the Germansen Landing–Manson Creek area, British Columbia. British Columbia Ministry of Energy, Mines and Petroleum Resources, British Columbia Geological Survey, Bulletin 91, scale 1:100 000.

Halleran, A.A.D., 1980. Petrology, mineralogy and origin of the niobium-bearing Lonnie carbonatite complex of the Manson Creek area, British Columbia. Unpublished B.Sc. thesis, University of British Columbia, 41 p.

Hankinson, J.D., 1958. The Lonnie group columbium deposit, Unpublished B.Sc. thesis, University of British Columbia, 32 p.

Hawkes, H. E., (1976). The downstream dilution of stream sediment anomalies. Journal of Geochemical Exploration, 6, pp. 345-358.

Helmel, A., 2012. Rara Terra Minerals receives soil geochemical survey results from Lonnie Project. Press release <http://www.raraterra.com/investors/news/2012/mar27/> accessed October 2013.

Mackay, D.A.R. and Simandl, G.J., 2014a. Portable x-ray fluorescence to optimize stream sediment chemistry and indicator mineral surveys, case 1: Carbonatite-hosted Nb deposits, Aley carbonatite, British Columbia, Canada. In: Geological Fieldwork 2013, British Columbia Ministry of Energy and Mines, British Columbia Geological Survey Paper 2014-1, this volume.

Mackay, D.A.R. and Simandl, G.J., 2014b. Portable x-ray fluorescence to optimize stream sediment chemistry and indicator mineral surveys, case 2: Carbonatite-hosted REE deposits, Wicheeda Lake, British Columbia, Canada. In: Geological Fieldwork 2013, British Columbia Ministry of Energy and Mines, British Columbia Geological Survey Paper 2014-1,this volume.

Mariano, A.N. 1989a. Economic geology of rare earth minerals. In: Lipman B.R. and McKay G.A. (Eds.) Geochemistry and Mineralogy of Rare Earth Elements: Reviews in Mineralogy, Volume 21, pp. 303-337.

Mariano, A.N. 1989b. Nature of economic mineralization in carbonatites and related rocks. In: Bell, K. (Ed.) Carbonatites: Genesis and Evolution. Unwin Hyman, London, pp. 149-176.

May, W.E. and Rumble, J. Jr, 2003. Certificate of analysis - standard reference material 2780. National Institute of Standards and

Technology, Gaithersburg, USA, 4 p.
McClenaghan, M.B., 2011 Overview of processing methods for recovery of indicator minerals from sediment and bedrock samples. Workshop in the 25th International Applied Geochemistry Symposium, Vuorimiesyhdistys, Rovaniemi, Finland, pp. 1-6.
Mongolia Central Geological Laboratory, 2006. Certified Reference Material "TRLK" Rare Earth Ore "CGL 124" Certificate of Analysis. Ulaanbaatar, Mongolia, 6 p.
Pell, J., 1994. Carbonatites, nepheline syenites, kimberlites and related rocks in British Columbia. British Columbia Ministry of Energy, Mines and Petroleum Resources, British Columbia Geological Survey, Bulletin 88, 136 p.
Rowe, R.B., 1958. Niobium (columbium) deposits of Canada. Geological Survey of Canada, Economic Geology Series 18, 103p.
Simandl, G.J., Prussin, E.A., and Brown, N., 2012. Specialty metals in Canada. British Columbia Ministry of Energy and Mines, British Columbia Geological Survey, Open File 2012-7, 48 p.
Simandl, G.J., Reid, H.M., and Ferri, F., 2013a. Geological setting of the Lonnie niobium deposit, British Columbia, Canada. In: Geological Fieldwork 2012, British Columbia Ministry of Energy, Mines and Natural Gas, British Columbia Geological Survey Paper 2013-1, pp. 127-138.
Simandl, G.J., Fajber, R., Paradis, S., and Simandl, L.J., 2013b. Exploration for sedimentary phosphate (± REE) deposits using handheld XRF – An orientation survey. Geochemistry: Exploration, Environment, Analysis. Available online: http://dx.doi.org/10.1144/geochem2012-180.
Simandl, G.J., Stone, R.S., Paradis, S., Fajber, R., Reid, H.M., and Grattan, K., 2013c. An assessment of a handheld X-ray fluorescence instrument for use in exploration and development with an emphasis on REEs and related specialty metals. Mineralium Deposita. Available online: http://link.springer.com/article/10.1007/s00126-013-0493-0.
Steger, H.F. and Bowman, W.S., 1981. OKA-1: a certified niobium reference ore. CANMET Report 81-1E, Canada Centre for Mineral and Energy Technology, Ottawa, Canada, 16 p.
Thompson, R.M., 1955. Lonnie. British Columbia Department of Mines, Minister of Mines Annual Report 1954, A96-A97.
Woolley, A.R. and Kjarsgaard, B.A., 2008. Carbonatite occurrences of the world; map and database. Geological Survey of Canada, Open File 5796, scale 1:19 000 000.